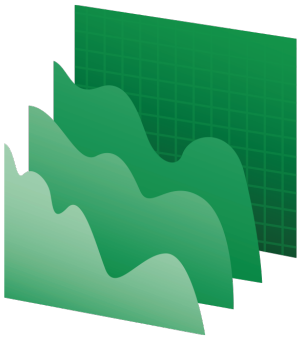

Match-up database Analyses Report

SMAP-L3-JPL-V4-8DAY-RUNNING-60KM

TSG-GOSUD-Research-vessel

Mediterranean Sea

prepared by the Pi-MEP Consortium

May 21, 2018

Contents

1 Overview **3**

2 The MDB file datasets **4**
2.1 Satellite SSS product . . . 4
2.1.1 SMAP-L3-JPL-V4-8DAY-RUNNING-60KM . . . 4
2.2 In situ SSS dataset . . . 4
2.3 Auxiliary geophysical datasets . . . 5
2.3.1 CMORPH . . . 5
2.3.2 ASCAT . . . 6
2.3.3 ISAS . . . 6
2.3.4 World Ocean Atlas Climatology . . . 7
2.4 Overview of the Match-ups generation method . . . 7
2.4.1 In Situ/Satellite data filtering . . . 7
2.4.2 In Situ/Satellite Co-localization . . . 7
2.4.3 MDB pair Co-localization with auxiliary data and complementary information . . . 8
2.4.4 Content of the Match-Up NetCDF files . . . 9
2.5 MDB characteristics for the particular in situ/satellite pairs . . . 13
2.5.1 Number of paired SSS data as a function of time and distance to coast . . . 13
2.5.2 Histograms of the SSS match-ups . . . 13
2.5.3 Distribution in situ SSS depth in match-ups pairs . . . 14
2.5.4 Spatial Distribution of Match-ups . . . 14
2.5.5 Histograms of the spatial and temporal lags of the match-ups pairs . . . 15

3 MDB file Analyses **15**
3.1 Spatial Maps of the Temporal mean and STD of in situ and satellite SSS and of the difference (ΔSSS) . . . 15
3.2 Time series of the monthly averaged mean and STD of in situ and satellite SSS and of the (ΔSSS) . . . 16
3.3 Zonally-averaged Time-mean and temporal STD of in situ and satellite SSS and of the ΔSSS . . . 17
3.4 Scatterplots of satellite vs in situ SSS by latitudinal bands . . . 19
3.5 Time series of the monthly averaged mean and STD of the ΔSSS sorted by latitudinal bands . . . 20
3.6 ΔSSS sorted as function of geophysical conditions . . . 20

4 Summary **23**

Acronym

Aquarius	NASA/CONAE Salinity mission
ASCAT	Advanced Scatterometer
ATBD	Algorithm Theoretical Baseline Document
BLT	Barrier Layer Thickness
CMORPH	CPC MORPHing technique
CTD	Instrument used to measure the conductivity, temperature, and pressure of seawater
DM	Delayed Mode
EO	Earth Observation
ESA	European Space Agency
FTP	File Transfer Protocol
GOSUD	Global Ocean Surface Underway Data
GTMBA	The Global Tropical Moored Buoy Array
Ifremer	Institut français de recherche pour l'exploitation de la mer
IPEV	Institut polaire français Paul-Émile Victor
IQR	Interquartile range
ISAS	In Situ Analysis System
L2	Level 2
LEGOS	Laboratoire d'Etudes en Géophysique et Océanographie Spatiales
LOCEAN	Laboratoire d'Océanographie et du Climat : Expérimentations et Approches Numériques
LOPS	Laboratoire d'Océanographie Physique et Spatiale
MDB	Match-up database
MEOP	Marine Mammals Exploring the Oceans Pole to Pole
MLD	Mixed Layer Depth
NRT	Near Real Time
Pi-MEP	Pilot Mission Exploitation Platform
PIRATA	Prediction and Researched Moored Array in the Atlantic
QC	Quality control
R_{sat}	Spatial resolution of the satellite SSS product
RAMA	Research Moored Array for African-Asian-Australian Monsoon Analysis and Prediction
RR	Rain rate
SAMOS	Shipboard Automated Meteorological and Oceanographic System
SMAP	Soil Moisture Active Passive (NASA mission)
SMOS	Soil Moisture and Ocean Salinity (ESA mission)
SSS	Sea Surface Salinity
SSS_{insitu}	In situ SSS data considered for the match-up
SSS_{SAT}	Satellite SSS product considered for the match-up
ΔSSS	Difference between satellite and in situ SSS at colocalized point ($\Delta SSS = SSS_{SAT} - SSS_{insitu}$)
SST	Sea Surface Temperature
STD	Standard deviation
Survostral	SURVeillance de l'Océan AuSTRAL (Monitoring the Southern Ocean)
TAO	Tropical Atmosphere Ocean
TSG	Thermosalinograph

1 Overview

In this report, we present systematic analyses of the Match-up DataBase (MDB) files generated by the Pi-MEP platform within the following Pi-MEP region and for the below pair of Satellite/In situ SSS data:

- Pi-MEP region: Mediterranean Sea
- SSS satellite product (SSS_{SAT}): SMAP-L3-JPL-V4-8DAY-RUNNING-60KM
- In situ dataset (SSS_{Insitu}): TSG-GOSUD-Research-vessel

In the following, $\Delta SSS = SSS_{SAT} - SSS_{Insitu}$ denotes the difference between the satellite and in situ SSS at the colocalized points that form the MDB.

This report presents successively:

The MDB file DataSets (Section 2)

- A short description of the satellite SSS product considered in the match-up (2.1)
- A short description of the In situ SSS dataset considered in the match-up (2.2)
- A short description of the auxiliary geophysical datasets co-localized with SSS pairs (2.3)
- An overview of how the Match-ups were evaluated (2.4)
- An overview of the MDB characteristics for the particular in situ/satellite pairs (2.5)

The major results of the MDB file Analyses (Section 3)

- Spatial Maps of the Time-mean and temporal STD of in situ and satellite SSS and of the ΔSSS (3.1)
- Time series of the monthly averaged mean and STD of in situ and satellite SSS and of the ΔSSS (3.2)
- Zonally-averaged Time-mean and temporal STD of in situ and satellite SSS and of the ΔSSS (3.3)
- Scatterplots of satellite vs in situ SSS by latitudinal bands (3.4)
- Time series of the monthly averaged mean and STD of the ΔSSS sorted by latitudinal bands (3.5)
- ΔSSS sorted as function of geophysical conditions (3.6)

All analyses are conducted over the Pi-MEP Region specified above and over the full satellite SSS product period.

2 The MDB file datasets

2.1 Satellite SSS product

2.1.1 SMAP-L3-JPL-V4-8DAY-RUNNING-60KM

This is the PI-produced JPL SMAP-SSS V4.0 CAP, 8-day running mean, level 3 mapped, sea surface salinity product from the NASA Soil Moisture Active Passive (SMAP) observatory. It is based on the Combined Active-Passive (CAP) retrieval algorithm developed at JPL originally in the context of Aquarius/SAC-D and now extended to SMAP. Daily data files for this product are based on SSS averages spanning an 8-day moving time window. Associated file variables include: derived SSS and wind speed data from SMAP and ancillary surface salinity from HYCOM. SMAP data begins on April 1, 2015 and is ongoing, with a 7-day latency in processing and availability. L3 products are global in extent and gridded at 0.25° x 0.25° with an approximate spatial resolution of 60 km. Improvements with this V4.0 dataset include: addition of estimated SSS uncertainty, improvement of TB correction for high latitudes, modification of the land correction range to 1000 km from coast, change of the ancillary wind source from NCEP GDAS to NCEP GFS resulting in significant improvements in SSS retrievals near storms, extension of the range of SSS retrievals to 45 PSU, and SSS retrievals also for large inland seas. The SMAP satellite is in a near-polar orbit at an inclination of 98 degrees and an altitude of 685 km. It has an ascending node time of 6 pm and is sun-synchronous. With its 1000km swath, SMAP achieves global coverage in approximately 3 days, but has an exact orbit repeat cycle of 8 days. On board instruments include a highly sensitive L-band radiometer operating at 1.41GHz and an L-band 1.26GHz radar sensor providing complementary active and passive sensing capabilities. Malfunction of the SMAP scatterometer on 7 July, 2015, has necessitated the use of collocated wind speed for the surface roughness correction required for the surface salinity retrieval.

Table 1: Satellite SSS product characteristics

SMAP-L3-JPL-V4-8DAY-RUNNING-60KM	
Spatial resolution	∼60 km gridded at 0.25° x 0.25°
Temporal resolution	8 Day
Temporal coverage	From 2015-04-01 to now
Spatial coverage	Global [-180 180 -90 90]
Data Provider	JPL Climate Oceans and Solid Earth group
Release Date	2018-02-22
Version	4
User Guide	JPL_SMAP-SSS-UsersGuide_V4.pdf
Documentation	ftp://podaac-ftp.jpl.nasa.gov/allData/smap/docs/JPL-CAP_V4/
DOI	http://doi.org/10.5067/SMP40-3TPCS

2.2 In situ SSS dataset

The TSG-GOSUD-Research-vessel dataset correspond to French research vessels that have been collecting thermo-salinometer (TSG) data since the early 2000 in contribution to the GOSUD program. The set of homogeneous instruments is permanently monitored and regularly calibrated. Water samples are taken on a daily basis by the crew and later analysed in the laboratory. The careful calibration and instrument maintenance, complemented with a rigorous adjustment on water samples lead to reach an accuracy of a few 10^{-2} PSS in salinity. This delayed mode

dataset (Gaillard et al. (2015)) is updated annually and freely available here. Adjusted values when available and only collected TSG data that exhibit quality flags=1 and 2 were used.

2.3 Auxiliary geophysical datasets

Additional EO datasets are used to characterize the geophysical conditions at the in situ/satellite SSS pair measurement locations and time, and 10 days prior the measurements to get an estimate of the geophysical condition and history. As discussed in Boutin et al. (2016), the presence of vertical gradients in, and horizontal variability of, sea surface salinity indeed complicates comparison of satellite and in situ measurements. The additional EO data are used here to get a first estimates of conditions for which L-band satellite SSS measured in the first centimeters of the upper ocean within a 50-150 km diameter footprint might differ from pointwise in situ measurements performed in general between 10 and 5 m depth below the surface. The spatio-temporal variability of SSS within a satellite footprint (50–150 km) is a major issue for satellite SSS validation in the vicinity of river plumes, frontal zones, and significant precipitation. Rainfall can in some cases produce vertical salinity gradients exceeding 1 pss m^{-1}; consequently, it is recommended that satellite and in situ SSS measurements less than 3–6 h after rain events should be considered with care when used in satellite calibration/validation analyses. To identify such situation, the Pi-MEP test platform is first using CMORPH products to characterize the local value and history of rain rate and ASCAT gridded data are used to characterize the local surface wind speed and history.

2.3.1 CMORPH

Precipitation are estimated using the CMORPH 3-hourly products at 1/4° resolution (Joyce et al. (2004)). CMORPH (CPC MORPHing technique) produces global precipitation analyses at very high spatial and temporal resolution. This technique uses precipitation estimates that have been derived from low orbiter satellite microwave observations exclusively, and whose features are transported via spatial propagation information that is obtained entirely from geostationary satellite IR data. At present NOAA incorporate precipitation estimates derived from the passive microwaves aboard the DMSP 13, 14 and 15 (SSM/I), the NOAA-15, 16, 17 and 18 (AMSU-B), and AMSR-E and TMI aboard NASA's Aqua, TRMM and GPM spacecraft, respectively. These estimates are generated by algorithms of Ferraro (1997) for SSM/I, Ferraro et al. (2000) for AMSU-B and Kummerow et al. (2001) for TMI. Note that this technique is not a precipitation estimation algorithm but a means by which estimates from existing microwave rainfall algorithms can be combined. Therefore, this method is extremely flexible such that any precipitation estimates from any microwave satellite source can be incorporated.

With regard to spatial resolution, although the precipitation estimates are available on a grid with a spacing of 8 km (at the equator), the resolution of the individual satellite-derived estimates is coarser than that - more on the order of 12 x 15 km or so. The finer "resolution" is obtained via interpolation.

In effect, IR data are used as a means to transport the microwave-derived precipitation features during periods when microwave data are not available at a location. Propagation vector matrices are produced by computing spatial lag correlations on successive images of geostationary satellite IR which are then used to propagate the microwave derived precipitation estimates. This process governs the movement of the precipitation features only. At a given location, the shape and intensity of the precipitation features in the intervening half hour periods between microwave scans are determined by performing a time-weighting interpolation between microwave-derived features that have been propagated forward in time from the previous microwave observation and

those that have been propagated backward in time from the following microwave scan. NOAA refer to this latter step as "morphing" of the features.

For the present Pi-MEP products, we only considered the 3-hourly products at 1/4 degree resolution. The entire CMORPH record (December 2002-present) for 3-hourly, 1/4 degree lat/lon resolution can be found at: ftp://ftp.cpc.ncep.noaa.gov/precip/CMORPH_V1.0/RAW/. CMORPH estimates cover a global belt (-180°W to 180°E) extending from 60°S to 60°N latitude and are available for the complete period of the Pi-MEP core datasets (Jan 2010-now).

2.3.2 ASCAT

Advanced SCATterometer (ASCAT) daily data produced and made available at Ifremer/CERSAT on a 0.25°x0.25° resolution grid (Bentamy and Fillon (2012)) since November 2008 are used to characterize the mean daily wind at the match-up pair location as well as the wind history during the 10-days period preceding the in situ measurement date. These wind fields are calculated based on a geostatistical method with external drift. Remotely sensed data from ASCAT are considered as observations while those from numerical model analysis (ECMWF) are associated with the external drift. The spatial and temporal structure functions for wind speed, zonal and meridional wind components are estimated from ASCAT retrievals. Furthermore, the new procedure includes a temporal interpolation of the retrievals based on the complex empirical orthogonal function (CEOF) approach, in order to enhance the sampling length of the scatterometer observations. The resulting daily wind fields involves the main known surface wind patterns as well as some variation modes associated with temporal and spatial moving features. The accuracy of the gridded winds was investigated through comparisons with moored buoy data in Bentamy et al. (2012) and resulted in rms differences for wind speed and direction are about 1.50 $m.s^{-1}$ and 20°.

2.3.3 ISAS

The In Situ Analysis System (ISAS), as described in Gaillard et al. (2016) is a data based reanalysis of temperature and salinity fields over the global ocean. It was initially designed to synthesize the temperature and salinity profiles collected by the ARGO program. It has been later extended to accommodate all type of vertical profile as well as time series. ISAS gridded fields are entirely based on in-situ measurements. The methodology and configuration have been conceived to preserve as much as possible the data information content and resolution. ISAS is developed and run in a research laboratory (LOPS) in close collaboration with Coriolis, one of ARGO Global Data Assembly Center and unique data provider for the Mercator operational oceanography system. At the moment the period covered starts in 2002 and only the upper 2000m are considered. The gridded fields were produced over the global ocean 70°N–70°S on a 1/2° grid by the ISAS project with datasets downloaded from the Coriolis data center (for more details on ISAS see Gaillard et al. (2009)). In the PiMEP, the product in used is the INSITU_GLO_TS_OA_NRT_OBSERVATIONS_013_002_a v6.2 NRT derived at the Coriolis data center and provided by Copernicus (www.marine.copernicus.eu/documents/PUM/CMEMS-INS-PUM-013-002-ab.pdf). The major contribution to the data set is from Argo array of profiling floats, reaching an approximate resolution of one profile every 10-days and every 3-degrees over the Satellite SSS period (http://www.umr-lops.fr/SNO-Argo/Products/ISAS-T-S-fields/); in this version SSS from thermosalinographs from ship of opportunity are not used, so that we can consider SMOS SSS validation using ship of opportunity measurements independent of ISAS. The ISAS optimal interpolation involves a structure function modeled as the sum of two Gaussian functions, each associated with specific time and space scales, resulting in a smoothing over typically 3 degrees. The smallest scale which can be retrieved with ISAS analysis is not smaller

than 300–500 km (Kolodziejczyk et al. (2015)). For validation purpose, the ISAS monthly SSS fields at depth level 5 m are collocated and compared with the satellite SSS products and included in the PiMEP MDB files. In addition, the « percentage of variance » fields (PCTVAR) contained in the ISAS analyses provide information on the local variability of in situ SSS measurements within 1/2°x1/2° boxes.

2.3.4 World Ocean Atlas Climatology

The World Ocean Atlas 2013 version 2 (WOA13 V2) is a set of objectively analyzed (1° grid) climatological fields of in situ temperature, salinity and other variables provided at standard depth levels for annual, seasonal, and monthly compositing periods for the World Ocean. It also includes associated statistical fields of observed oceanographic profile data interpolated to standard depth levels on 5°, 1°, and 0.25° grids. We use these fields in complement to ISAS to characterize the climatological fields (monthly mean and std) at the match-up pairs location and date.

2.4 Overview of the Match-ups generation method

The match-up production is basically a three steps process:

1. preparation of the input in situ and satellite data, and,
2. co-localization of satellite products with in situ SSS measurements.
3. co-localization of the in situ/satellite pair with auxiliary information.

In the following, we successively detail the approaches taken for these different steps.

2.4.1 In Situ/Satellite data filtering

The first step consist in filtering TSG-GOSUD-Research-vesselin situ dataset using the quality flags as described in 2.2 so that only valid salinity data remains in the produced match-ups.

For high-spatial resolution in situ SSS measurements such as the Thermo-SalinoGraph (TSG) SSS data from research vessels, Voluntary Observing Ships (VOS) or sailing ships, as well as SSS data from surface drifters, an additional spatial-filtering step is performed on the in situ data that will be in fine compared to the satellite SSS products. If R_{sat} is the spatial resolution of the satellite SSS product (L2 to L3-L4), we keep the in situ data at the original spatial resolution but we also estimate for all spatio-temporal samples a running median filtered SSS applied to all neighbouring in situ SSS data acquired within a distance of $R_{sat}/2$ from a given in situ acquisition. Both the original and the filtered data are finally stored in the MDB files.

Only for satellite L2 SSS data, a third step consist in filtering spurious data using the flags and associated recommendation as provided by the official data centers and described in 2.1.

2.4.2 In Situ/Satellite Co-localization

In this step, each SSS satellite acquisition is co-localized with the filtered in situ measurements. The method used for co-localization differ if the satellite SSS is a swath product (so-called Level 2-types) or a time-space composite product (so-called Level 3/level 4-types).

- For L2 SSS swath data :

  If R_{sat} is the spatial resolution of the satellite swath SSS product, for each in situ data sample collected in the Pi-MEP database, the platform searches for all satellite SSS data

found at grid nodes located within a radius of $R_{sat}/2$ from the in situ data location and acquired with a time-lag from the in situ measurement date that is less or equal than ± 6 hours. If several satellite SSS samples are found to meet these criteria, the final satellite SSS match-up point is selected to be the closest in time from the in situ data measurement date. The final spatial and temporal lags between the in situ and satellite data are stored in the MDB files.

- For L3 and L4 composite SSS products :

  If R_{sat} is the spatial resolution of the composite satellite SSS product and D the period over which the composite product was built (e.g., periods of 1, 7, 8, 9, 10, 18 days, 1 month, etc..) with central time to, for each in situ data sample collected in the Pi-MEP database during period D, the platform searches for all satellite SSS data of the composite product found at grid nodes located within a radius of $R_{sat}/2$ from the in situ data location. If several satellite SSS product samples are found to meet these criteria, the final satellite SSS match-up point is chosen to be the composite SSS with central time to which is the closest in time from the in situ data measurement date. The final spatial and temporal lags between the in situ and satellite data are stored in the MDB files.

2.4.3 MDB pair Co-localization with auxiliary data and complementary information

MDB data consist of satellite and in-situ SSS pair datasets but also of auxiliary geophysical parameters such as local and history of wind speed and rain rates, as well as various information (climatology, distance to coast, mixed layer depth, barrier layer thickness, etc) that can be derived from in situ data and which are included in the final match-up files. The collocation of auxiliary parameters and additional information is done for each filtered in-situ SSS measurement contained in the match-up files as follows :

If t_{insitu} is the time/date at which the in situ measurement is performed, we collect:

- The ASCAT wind speed product of the same day than t_{insitu} found at the ASCAT 1/4° grid node with closest distance from the in situ data location and the time series of the ASCAT wind speed at the same node for the 10 days prior the in situ measurement day.

- If the in situ data is located within the 60°N-60°S band, we select the CMORPH 3-hourly product the closest in time from tin situ and found at the CMORPH 1/4° grid node with closest distance from the in situ data location. We then store the time series of the CMORPH rain rate at the same node for the 10 days prior the in situ measurement time.

For the given month/year of the in situ data, we select the ISAS and WOA fields for the same month (and same year for ISAS fields) and take the SSS analysis (monthly mean, std) found at the grid node the closest from the in situ measurement.

The distance from the in situ SSS data location to the nearest coast is evaluated and provided in kms. We use a distance-to-coast map derived by CLS with a spatial resolution of 1/16° that we re-gridded at 1/4° resolution taking the minimum value of all 1/16° observations found in the 1/4° grid cell.

When vertical profiles of S and T are made available from the in situ measurements used to build the match-up (Argo or sea mammals), the following variables are included into each satellite/in situ match-up file:

1. The vertical distribution of pressure at which the profile were measured,

2. The vertical S(z) and T(z) profiles,

3. The vertical potential density anomaly profile $\sigma_0(z)$,

4. The Mixed Layer Depth (MLD). The MLD is defined here as the depth where the potential density has increased from the reference depth (10 meter) by a threshold equivalent to 0.2°C decrease in temperature at constant salinity: $\sigma_0 = \sigma_{010m} + \Delta\sigma_0$ with $\Delta\sigma_0 = \sigma_0(\theta_{10m} - 0.2, S_{10m}) - \sigma_0(\theta_{10m}, S_{10m})$ where θ_{10m} and S_{10m} are the temperature and salinity at the reference depth (i.e. 10 m) (de Boyer Montégut et al. (2004), de Boyer Montégut et al. (2007)).

5. The Top of the Thermocline Depth (TTD) is defined as the depth at which temperature decreases from its 10 m value by 0.2°C.

6. The Barrier Layer if present, is defined as the intermediate layer between the top of the thermocline and the bottom of the density mixed-layer and its thickness (BLT) is defined as the difference between the MLD and the TTD.

7. The vertical profile of the buoyancy frequency $N^2(z)$

The resulting match-ups files are serialized as NetCDF-4 files whose structure depends on the origin of the in-situ data they contain.

2.4.4 Content of the Match-Up NetCDF files

netcdf pimep-mdb_smap-l3-jpl-v4-8dr_tsg-gosud-research-vessel_20100116_v01 {
dimensions:
TIME_SAT = UNLIMITED ; // (1 currently)
TIME_TSG = 2190 ;
N_DAYS_WIND = 10 ;
N_3H_RAIN = 80 ;
STRING25 = 25 ;
STRING8 = 8 ;

variables:
float DATE_TSG(TIME_TSG) ;
DATE_TSG:long_name = ”Date of TSG” ;
DATE_TSG:units = ”days since 1990-01-01 00:00:00” ;
DATE_TSG:standard_name = ”time” ;
DATE_TSG:_FillValue = -999.f ;
float LATITUDE_TSG(TIME_TSG) ;
LATITUDE_TSG:long_name = ”Latitude of TSG” ;
LATITUDE_TSG:units = ”degrees_north” ;
LATITUDE_DRIFTER:valid_min = -90. ;
LATITUDE_TSG:valid_max = 90. ;
LATITUDE_TSG:standard_name = ”latitude” ;
LATITUDE_TSG:_FillValue = -999.f ;
float LONGITUDE_TSG(TIME_TSG) ;
LONGITUDE_TSG:long_name = ”Longitude of TSG” ;
LONGITUDE_TSG:units = ”degrees_east” ;
LONGITUDE_TSG:valid_min = -180. ;

LONGITUDE_TSG:valid_max = 180. ;
LONGITUDE_TSG:standard_name = ”longitude” ;
LONGITUDE_TSG:_FillValue = -999.f ;
float SSS_TSG(TIME_TSG) ;
SSS_TSG:long_name = ”Drifter SSS” ;
SSS_TSG:units = ”1” ;
SSS_TSG:salinity_scale = ”Practical Salinity Scale(PSS-78)” ;
SSS_TSG:standard_name = ”sea_water_salinity” ;
SSS_TSG:_FillValue = -999.f ;
float SST_TSG(TIME_TSG) ;
SST_TSG:long_name = ”Drifter SST” ;
SST_TSG:units = ”degree Celsius” ;
SST_TSG:standard_name = ”sea_water_temperature” ;
SST_TSG:_FillValue = -999.f ;
float SSS_TSG_FILTERED(TIME_TSG) ;
SSS_TSG_FILTERED:long_name = ”Drifter SSS median filtered at satellite spatial resolution” ;
SSS_TSG_FILTERED:units = ”1” ;
SSS_TSG_FILTERED:salinity_scale = ”Practical Salinity Scale(PSS-78)” ;
SSS_TSG_FILTERED:standard_name = ”sea_water_salinity” ;
SSS_TSG_FILTERED:_FillValue = -999.f ;
float SST_TSG_FILTERED(TIME_TSG) ;
SST_TSG_FILTERED:long_name = ”Drifter SST median filtered at satellite spatial resolution”
;
SST_TSG_FILTERED:units = ”degree Celsius” ;
SST_TSG_FILTERED:standard_name = ”sea_water_temperature” ;
SST_TSG_FILTERED:_FillValue = -999.f ;
float DISTANCE_TO_COAST_TSG(TIME_TSG) ;
DISTANCE_TO_COAST_TSG:long_name = ”Distance to coasts at TSG location” ;
DISTANCE_TO_COAST_TSG:units = ”km” ;
DISTANCE_TO_COAST_TSG:_FillValue = -999.f ;
float PLATFORM_NUMBER_TSG(TIME_TSG) ;
PLATFORM_NUMBER_TSG:long_name = ”TSG unique identifier” ;
PLATFORM_NUMBER_TSG:conventions = ”WMO float identifier : A9IIIII” ;
PLATFORM_NUMBER_TSG:units = ”1” ;
PLATFORM_NUMBER_TSG:_FillValue = -999.f ;
float DATE_Satellite_product(TIME_Sat) ;
DATE_Satellite_product:long_name = ”Central time of satellite SSS file” ;
DATE_Satellite_product:units = ”days since 1990-01-01 00:00:00” ;
DATE_Satellite_product:standard_name = ”time” ;
float LATITUDE_Satellite_product(TIME_TSG) ;
LATITUDE_Satellite_product:long_name = ”Satellite product latitude at TSG location” ;
LATITUDE_Satellite_product:units = ”degrees_north” ;
LATITUDE_Satellite_product:valid_min = -90. ;
LATITUDE_Satellite_product:valid_max = 90. ;
LATITUDE_Satellite_product:standard_name = ”latitude” ;
LATITUDE_Satellite_product:_FillValue = -999.f ;
float LONGITUDE_Satellite_product(TIME_TSG) ;
LONGITUDE_Satellite_product:long_name = ”Satellite product longitude at TSG location” ;
LONGITUDE_Satellite_product:units = ”degrees_east” ;

LONGITUDE_Satellite_product:valid_min = -180. ;
LONGITUDE_Satellite_product:valid_max = 180. ;
LONGITUDE_Satellite_product:standard_name = ”longitude” ;
LONGITUDE_Satellite_product:_FillValue = -999.f ;
float SSS_Satellite_product(TIME_TSG) ;
SSS_Satellite_product:long_name = ”Satellite product SSS at TSG location” ;
SSS_Satellite_product:units = ”1” ;
SSS_Satellite_product:salinity_scale = ”Practical Salinity Scale(PSS-78)” ;
SSS_Satellite_product:standard_name = ”sea_surface_salinity” ;
SSS_Satellite_product:_FillValue = -999.f ;
float SST_Satellite_product(TIME_TSG) ;
SST_Satellite_product:long_name = ”Satellite product SST at TSG location” ;
SST_Satellite_product:units = ”degree Celsius” ;
SST_Satellite_product:standard_name = ”sea_surface_temperature” ;
SST_Satellite_product:_FillValue = -999.f ;
float Spatial_lags(TIME_TSG) ;
Spatial_lags:long_name = ”Spatial lag between TSG location and satellite SSS product pixel center” ;
Spatial_lags:units = ”km” ;
Spatial_lags:_FillValue = -999.f ;
float Time_lags(TIME_TSG) ;
Time_lags:long_name = ”Temporal lag between TSG time and satellite SSS product central time” ;
Time_lags:units = ”days” ;
Time_lags:_FillValue = -999.f ;
float ROSSBY_RADIUS_at_TSG(TIME_TSG) ;
ROSSBY_RADIUS_at_TSG:long_name = ”Baroclinic Rossby radius of deformation (Chelton et al., 1998) at TSG location” ;
ROSSBY_RADIUS_at_TSG:units = ”km” ;
ROSSBY_RADIUS_at_TSG:_FillValue = -999.f ;
float Ascat_daily_wind_at_TSG(TIME_TSG) ;
Ascat_daily_wind_at_TSG:long_name = ”Daily Ascat wind speed module at TSG location” ;
Ascat_daily_wind_at_TSG:units = ”m/s” ;
Ascat_daily_wind_at_TSG:_FillValue = -999.f ;
float CMORPH_3h_Rain_Rate_at_TSG(TIME_TSG) ;
CMORPH_3h_Rain_Rate_at_TSG:long_name = ”3-hourly CMORPH rain rate at TSG location” ;
CMORPH_3h_Rain_Rate_at_TSG:units = ”mm/3h” ;
CMORPH_3h_Rain_Rate_at_TSG:_FillValue = -999.f ;
float Ascat_10_prior_days_wind_at_TSG(TIME_TSG, N_DAYS_WIND) ;
Ascat_10_prior_days_wind_at_TSG:long_name = ”Prior 10 days time series of Ascat wind speed module at TSG location” ;
Ascat_10_prior_days_wind_at_TSG:units = ”m/s” ;
Ascat_10_prior_days_wind_at_TSG:_FillValue = -999.f ;
float CMORPH_10_prior_days_Rain_Rate_at_TSG(TIME_TSG, N_3H_RAIN) ;
CMORPH_10_prior_days_Rain_Rate_at_TSG:long_name = ”Prior 10 days times series of 3-hourly CMORPH Rain Rate at TSG location” ;
CMORPH_10_prior_days_Rain_Rate_at_TSG:units = ”mm/3h” ;
CMORPH_10_prior_days_Rain_Rate_at_TSG:_FillValue = -999.f ;

float SSS_ISAS_at_TSG(TIME_TSG) ;
SSS_ISAS_at_TSG:long_name = ”ISAS SSS (5m depth) at TSG location” ;
SSS_ISAS_at_TSG:units = ”1” ;
SSS_ISAS_at_TSG:salinity_scale = ”Practical Salinity Scale(PSS-78)” ;
SSS_ISAS_at_TSG:standard_name = ”sea_water_salinity” ;
SSS_ISAS_at_TSG:_FillValue = -999.f ;
float SSS_PCTVAR_ISAS_at_TSG(TIME_TSG) ;
SSS_PCTVAR_ISAS_at_TSG:long_name = ”Error on ISAS SSS (5m depth) at TSG location (% variance)” ;
SSS_PCTVAR_ISAS_at_TSG:units = ”%” ;
SSS_PCTVAR_ISAS_at_TSG:_FillValue = -999.f ;
float SSS_WOA13_at_TSG(TIME_TSG) ;
SSS_WOA13_at_TSG:long_name = ”WOA 2013 (DECAV-1deg) SSS (0m depth) at TSG location” ;
SSS_WOA13_at_TSG:units = ”1” ;
SSS_WOA13_at_TSG:salinity_scale = ”Practical Salinity Scale(PSS-78)” ;
SSS_WOA13_at_TSG:standard_name = ”sea_surface_salinity” ;
SSS_WOA13_at_TSG:_FillValue = -999.f ;
float SSS_STD_WOA13_at_TSG(TIME_TSG) ;
SSS_STD_WOA13_at_TSG:long_name = ”WOA 2013 (DECAV-1deg) SSS STD (0m depth) at TSG location ” ;
SSS_STD_WOA13_at_TSG:units = ”1” ;
SSS_STD_WOA13_at_TSG:_FillValue = -999.f ;

// global attributes:
:Conventions = ”CF-1.6” ;
:title = ”TSG-GOSUD-Research-vesselMatch-Up Database” ;
:Satellite_product_name = ”SMOS L3 CATDS CECOS LOCEAN V2.1 9DAYS 25KM” ;
:Satellite_product_spatial_resolution = ”25 km” ;
:Satellite_product_temporal_resolution = ”9 days” ;
:Satellite_product_filename = ”v2.1/9days/SMOS_L3_DEBIAS_LOCEAN_AD_20100116_EASE_09d_25km_v00.nc” ;
:Match-Up_spatial_window_radius_in_km = 25. ;
:Match-Up_temporal_window_radius_in_days = 2. ;
:start_time = ”20100114T000005Z” ;
:stop_time = ”20100118T235026Z” ;
:northernmost_latitude = 77.676f ;
:sourthenmost_latitude = -66.423f ;
:westernmost_longitude = -179.219f ;
:easternmost_longitude = 179.199f ;
:geospatial_lat_units = ”degrees north” ;
:geospatial_lat_resolution = ”25 km” ;
:geospatial_lon_units = ”degrees east” ;
:geospatial_lon_resolution = ”25 km” ;
:institution = ”ESA-IFREMER-ODL” ;
:project_name = ”SMOS Pilote Mission Exploitation Platfrom (Pi-MEP) for salinity” ;
:project_url = ”https://pimep-project.odl.bzh” ;
:license = ”Pi-MEP data use is free and open” ;
:product_version = ”1.0” ;

:keywords = ”Oceans > Ocean Salinity > Sea Surface Salinity” ;
:acknowledgment = ”Please acknowledge the use of these data with the following statement: These data were provided by SMOS Pilote Mission Exploitation Platfrom (Pi-MEP) for salinity” ;
:source = ”v2.1/9days/SMOS_L3_DEBIAS_LOCEAN_AD_20100116_EASE_09d_25km_v00.nc” ;
:references = ”https://pimep-project.odl.bzh” ;
:history = ”Processed on 2018-04-18 using MDB_generator” ;
:date_created = ”2018-04-18 17:09:30” ;
}

2.5 MDB characteristics for the particular in situ/satellite pairs

2.5.1 Number of paired SSS data as a function of time and distance to coast

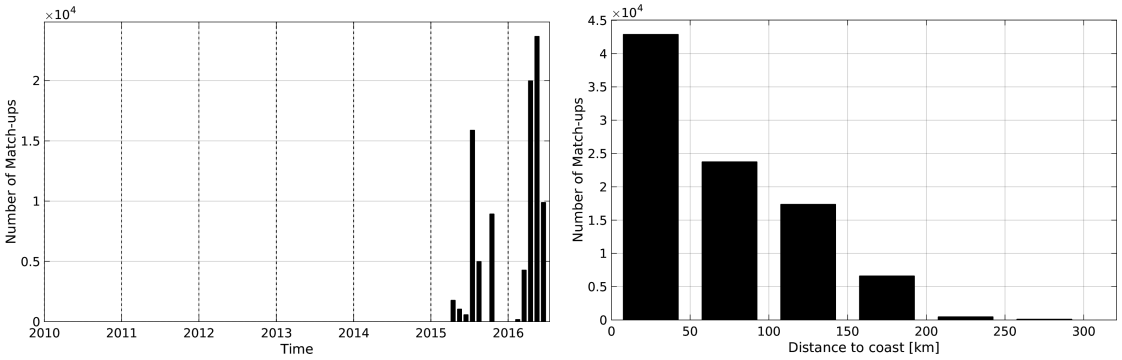

(a) (b)

Figure 1: Number of match-ups between TSG-GOSUD-Research-vessel and SMAP-L3-JPL-V4-8DAY-RUNNING-60KM SSS as a function of time (a) and as function of the distance to coast (b) over the Mediterranean Sea Pi-MEP region and for the full satellite product period.

2.5.2 Histograms of the SSS match-ups

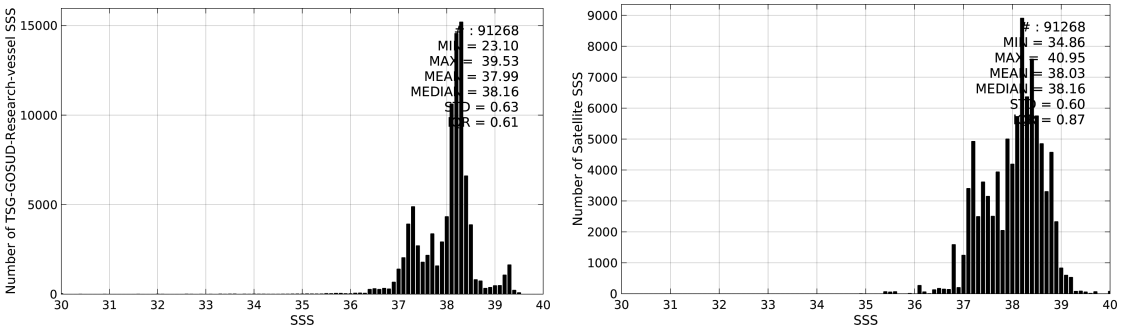

(a) (b)

Figure 2: Histograms of SSS from TSG-GOSUD-Research-vessel (a) and SMAP-L3-JPL-V4-8DAY-RUNNING-60KM (b) considering all match-up pairs per bins of 0.1 over the Mediterranean Sea Pi-MEP region and for the full satellite product period.

2.5.3 Distribution in situ SSS depth in match-ups pairs

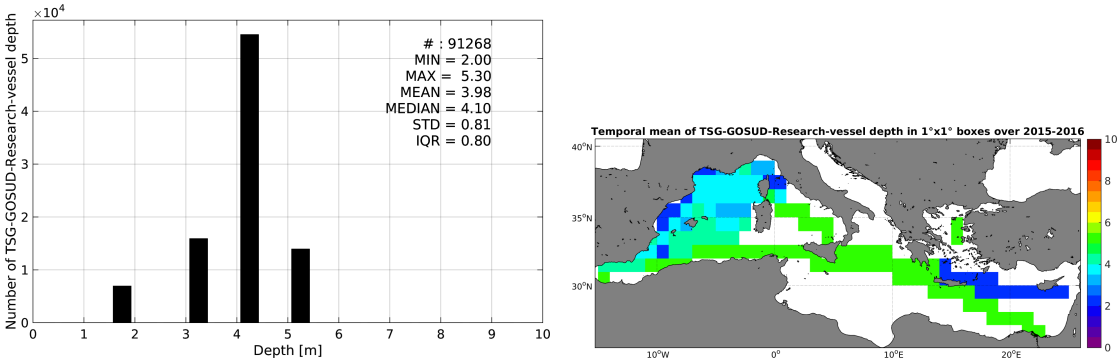

(a) (b)

Figure 3: Histograms of the depth of the upper level SSS measurements from TSG-GOSUD-Research-vessel in the Match-up DataBase for the Mediterranean Sea Pi-MEP region (a) and temporal mean spatial distribution of pressure of the in situ SSS data over 1°x1° boxes and for the full satellite product period (b).

2.5.4 Spatial Distribution of Match-ups

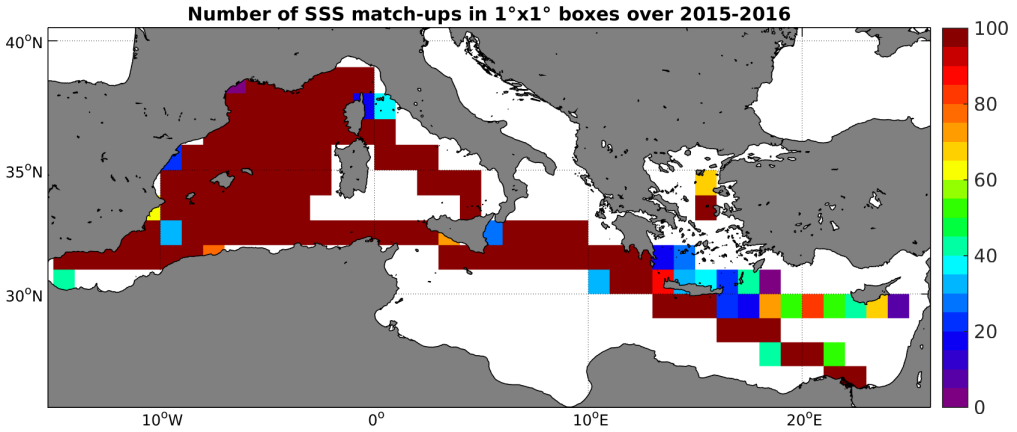

Figure 4: Number of SSS match-ups between TSG-GOSUD-Research-vessel SSS and the SMAP-L3-JPL-V4-8DAY-RUNNING-60KM SSS product for the Mediterranean Sea Pi-MEP region over 1°x1° boxes and for the full satellite product period.

2.5.5 Histograms of the spatial and temporal lags of the match-ups pairs

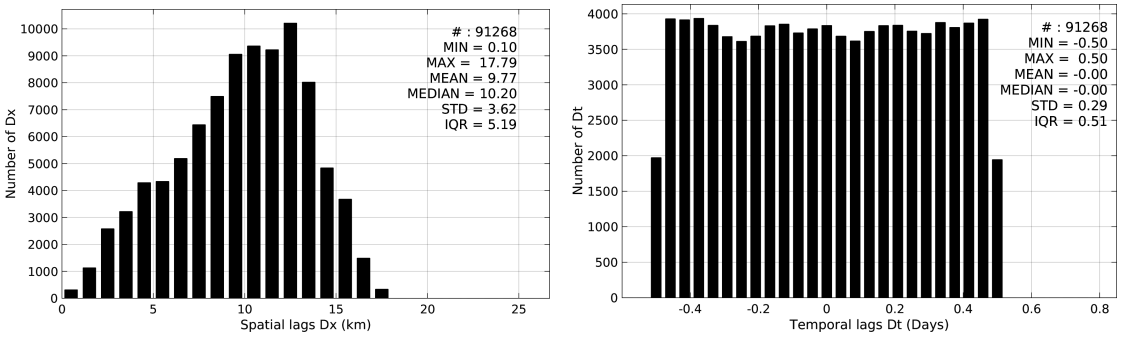

(a) (b)

Figure 5: Histograms of the spatial (a) and temporal (b) lags between the time of the TSG-GOSUD-Research-vessel measurements and the date of the corresponding SMAP-L3-JPL-V4-8DAY-RUNNING-60KM SSS product.

3 MDB file Analyses

3.1 Spatial Maps of the Temporal mean and STD of in situ and satellite SSS and of the difference (ΔSSS)

In Figure 6, we show maps of temporal mean (left) and standard deviation (right) of the SMAP-L3-JPL-V4-8DAY-RUNNING-60KM satellite SSS product (top) and of the TSG-GOSUD-Research-vessel in situ dataset at the collected Pi-MEP match-up pairs. The temporal mean and std are gridded over the full satellite product period and over spatial boxes of size 1°x1°.

At the bottom of Figure 6, the temporal mean (left) and standard deviation (right) of the differences between the satellite SSS product and in situ data found at match-up pairs, namely ΔSSS(Satellite -TSG-GOSUD-Research-vessel), is also gridded over the full satellite product period and over spatial boxes of size 1°x1°.

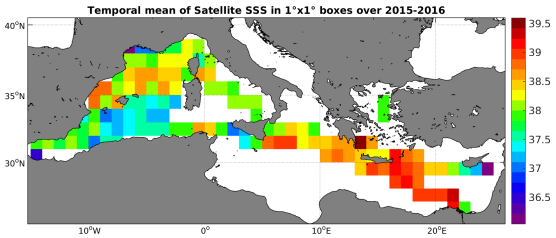

(a) MEAN(Satellite SSS)

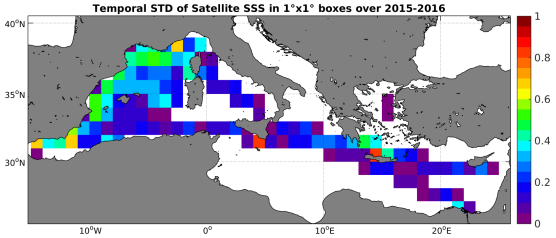

(b) STD(Satellite SSS)

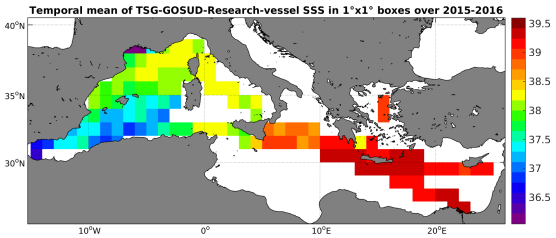

(c) MEAN(TSG-GOSUD-Research-vessel SSS)

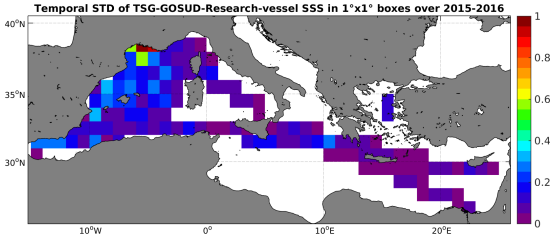

(d) STD(TSG-GOSUD-Research-vessel SSS)

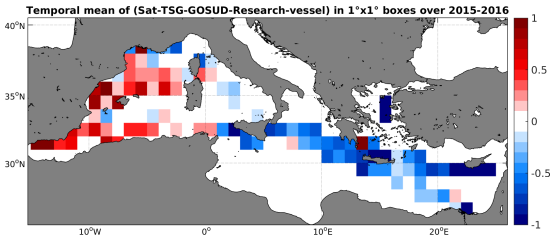

(e) MEAN(ΔSSS) (Satellite - TSG-GOSUD-Research-vessel)

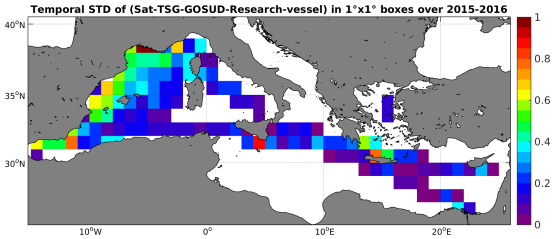

(f) STD(ΔSSS) (Satellite - TSG-GOSUD-Research-vessel)

Figure 6: Temporal mean (left) and STD (right) of SSS from SMAP-L3-JPL-V4-8DAY-RUNNING-60KM (top), TSG-GOSUD-Research-vessel (middle), and of ΔSSS (Satellite - TSG-GOSUD-Research-vessel). Only match-up pairs are used to generate these maps.

3.2 Time series of the monthly averaged mean and STD of in situ and satellite SSS and of the (ΔSSS)

In the top panel of Figure 7, we show the time series of the monthly averaged SSS estimated over the full Mediterranean Sea Pi-MEP region for both SMAP-L3-JPL-V4-8DAY-RUNNING-60KM satellite SSS product (in black) and the TSG-GOSUD-Research-vessel in situ dataset (in blue) at the collected Pi-MEP match-up pairs.

In the middle panel of Figure 7, we show the time series of the monthly averaged ΔSSS (Satellite - TSG-GOSUD-Research-vessel) for the collected Pi-MEP match-up pairs and estimated over the full Mediterranean Sea Pi-MEP region.

In the bottom panel of Figure 7, we show the time series of the monthly averaged standard deviation of the ΔSSS (Satellite - TSG-GOSUD-Research-vessel) for the collected Pi-MEP match-up pairs and estimated over the full Mediterranean Sea Pi-MEP region.

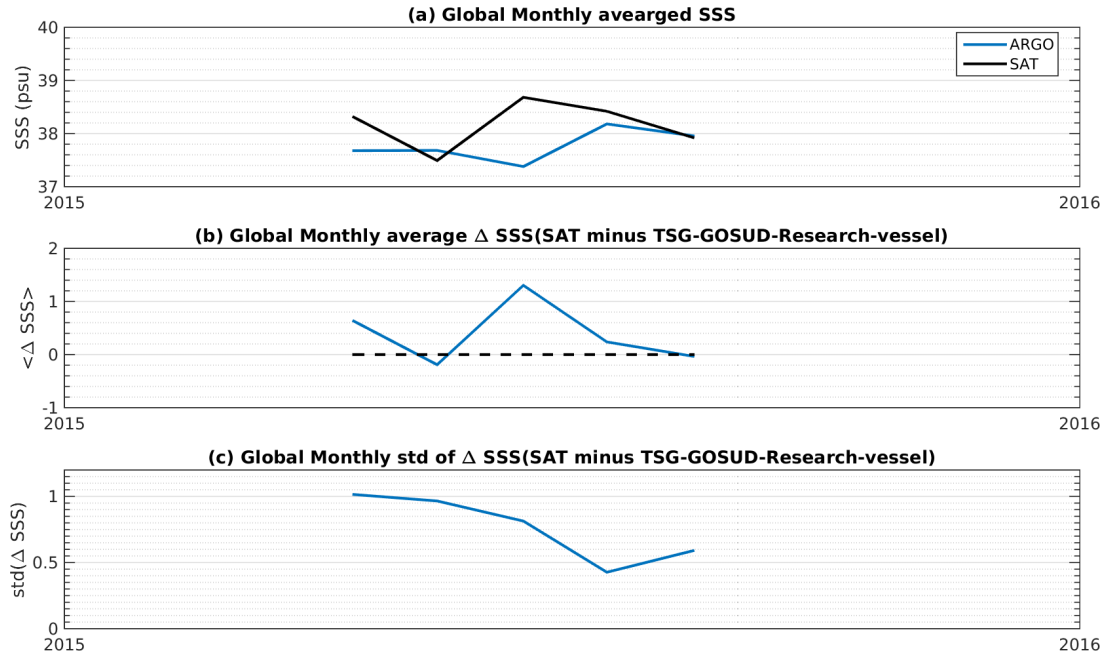

Figure 7: Time series of the monthly averaged mean SSS (top), mean ΔSSS (Satellite - TSG-GOSUD-Research-vessel) and STD of ΔSSS (Satellite - TSG-GOSUD-Research-vessel) over the Mediterranean Sea Pi-MEP region considering all match-ups collected by the Pi-MEP platform.

3.3 Zonally-averaged Time-mean and temporal STD of in situ and satellite SSS and of the ΔSSS

In Figure 8 left panel, we show the zonally averaged time-mean SSS estimated at the collected Pi-MEP match-up pairs for both SMAP-L3-JPL-V4-8DAY-RUNNING-60KM satellite SSS product (in black) and the TSG-GOSUD-Research-vessel in situ dataset (in blue). The time mean is evaluated over the full satellite SSS product period.

In the right panel of Figure 8, we show the zonally averaged time-mean ΔSSS (Satellite - TSG-GOSUD-Research-vessel) for all the collected Pi-MEP match-up pairs estimated over the full satellite product period.

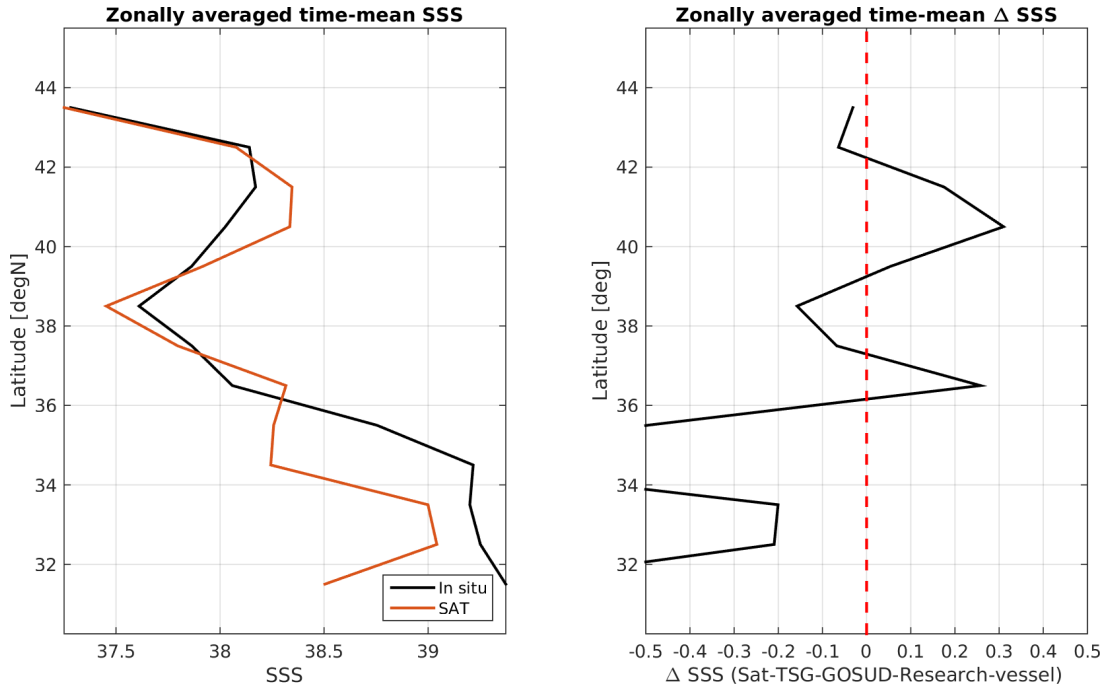

Figure 8: Left panel: Zonally averaged time mean SSS from SMAP-L3-JPL-V4-8DAY-RUNNING-60KM (black) and from TSG-GOSUD-Research-vessel (blue). Right panel: zonally averaged time-mean ΔSSS (Satellite - TSG-GOSUD-Research-vessel) for all the collected Pi-MEP match-up pairs estimated over the full satellite product period.

3.4 Scatterplots of satellite vs in situ SSS by latitudinal bands

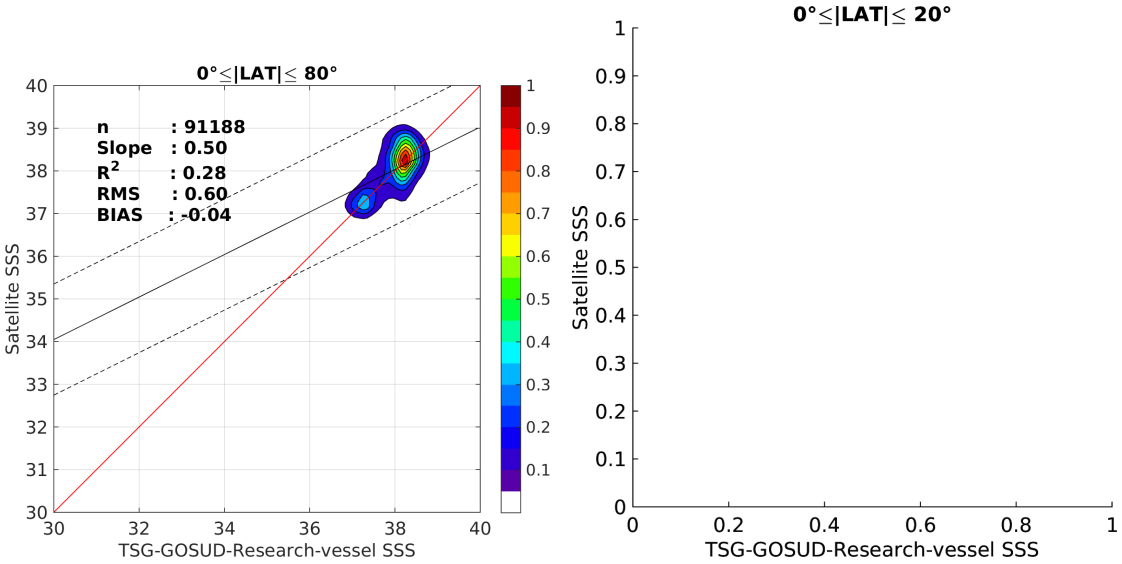

(a) $0° \leq |\text{LAT}| \leq 80°$

(b) $0° \leq |\text{LAT}| \leq 20°$

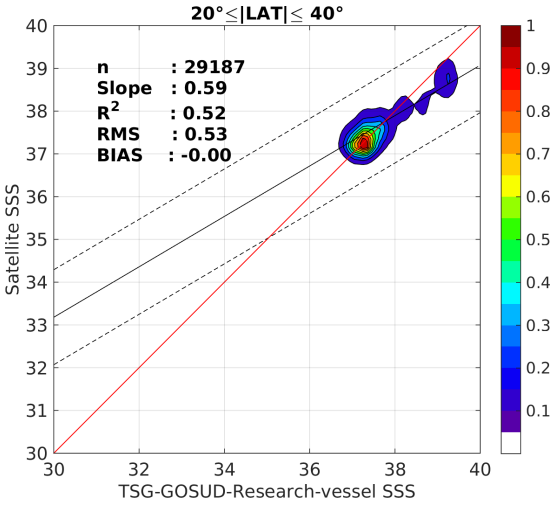

(c) $20° \leq |\text{LAT}| \leq 40°$

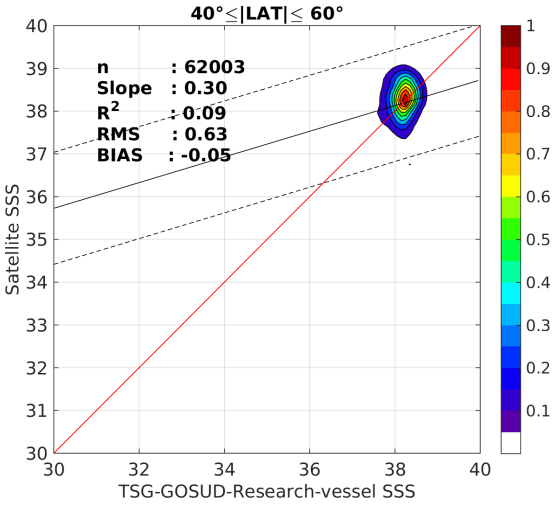

(d) $40° \leq |\text{LAT}| \leq 60°$

Figure 9: Contour maps of the concentration of SMAP-L3-JPL-V4-8DAY-RUNNING-60KM SSS (y-axis) versus TSG-GOSUD-Research-vessel SSS (x-axis) at match-up pairs for different latitude bands. For each plot, the red line shows x=y. The black thin and dashed lines indicate a linear fit through the data cloud and the ±95% confidence levels, respectively. The number match-up pairs n, the slope and R^2 coefficient of the linear fit, the root mean square (RMS) and the mean bias between satellite and in situ data are indicated for each latitude band in each plots.

3.5 Time series of the monthly averaged mean and STD of the ΔSSS sorted by latitudinal bands

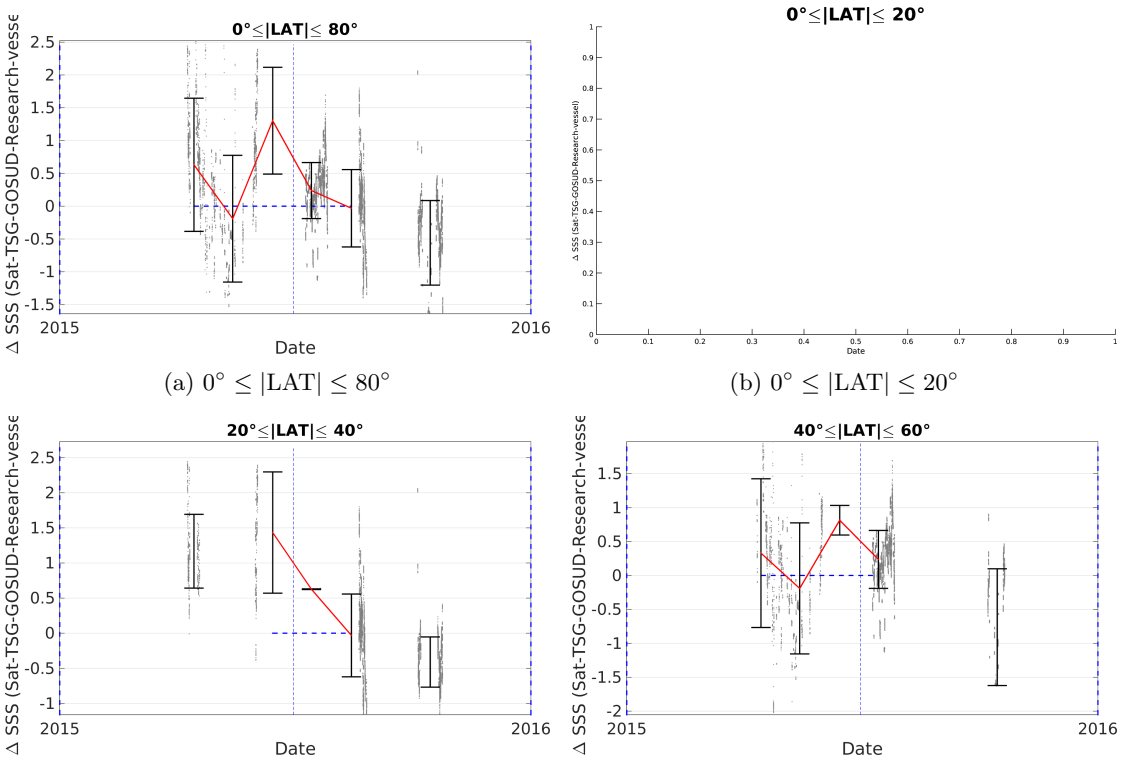

(a) $0° \leq |LAT| \leq 80°$

(b) $0° \leq |LAT| \leq 20°$

(c) $20° \leq |LAT| \leq 40°$

(d) $40° \leq |LAT| \leq 60°$

Figure 10: Monthly-average mean (red curves) ΔSSS (Satellite - TSG-GOSUD-Research-vessel) and ±1 STD (black vertical thick bars) as function of time for all the collected Pi-MEP match-up pairs estimated over the Mediterranean Sea Pi-MEP region and for the full satellite product period are shown for different latitude bands: (a) Latitude band 80°S-80°N, (b) latitude band 20°S-20°N, (c) Mid Latitude bands 40°S-20°S and 20°N-40°N and (d) Latitude bands 60°S-40°S and 40°N-60°N.

3.6 ΔSSS sorted as function of geophysical conditions

In Figure 11, we classify the match-up differences ΔSSS (Satellite - in situ) between SMAP-L3-JPL-V4-8DAY-RUNNING-60KM and TSG-GOSUD-Research-vessel SSS as function of the geophysical conditions at match-up points. The mean and std of ΔSSS (Satellite - TSG-GOSUD-Research-vessel) is thus evaluated as function of the

- in situ SSS values per bins of width 0.2,
- in situ SST values per bins of width 1°C,
- ASCAT daily wind values per bins of width 1 m/s,
- CMORPH 3-hourly rain rates per bins of width 1 mm/h, and,
- distance to coasts per bins of width 50 km.

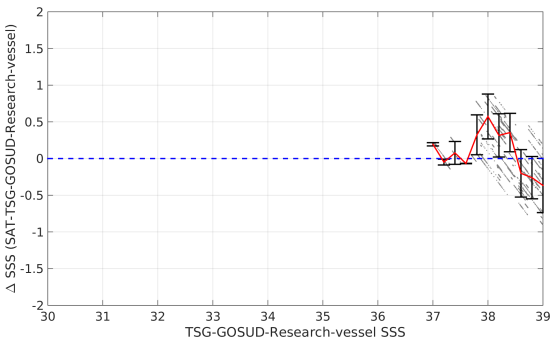

(a) TSG-GOSUD-Research-vessel SSS

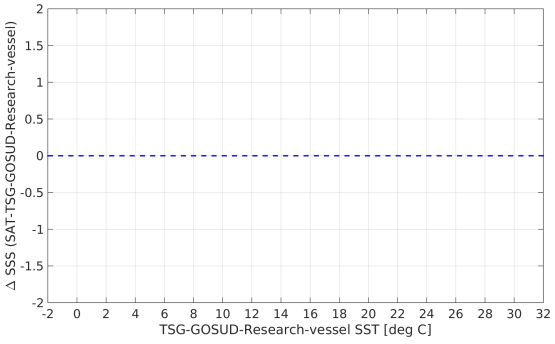

(b) TSG-GOSUD-Research-vessel SST

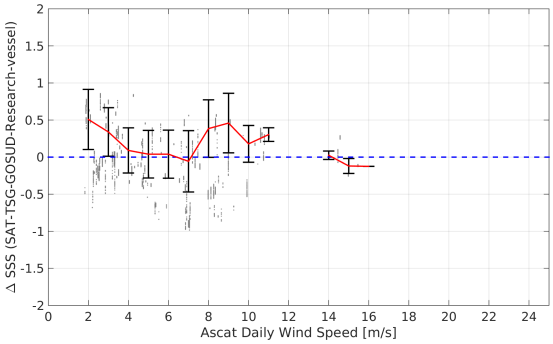

(c) ASCAT Wind Speed

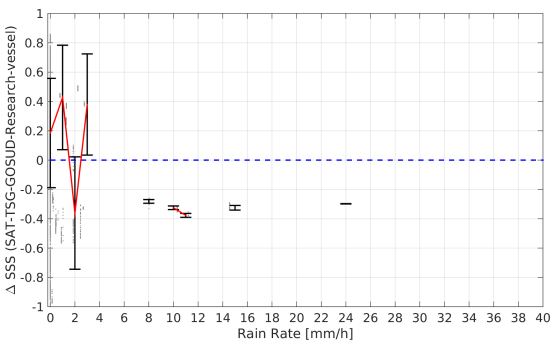

(d) CMORPH Rain rate

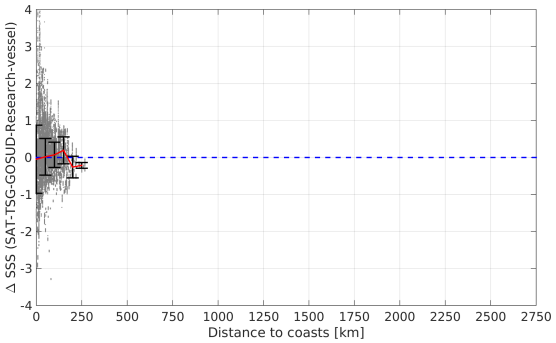

(e) Distance to coast

Figure 11: ΔSSS (Satellite - TSG-GOSUD-Research-vessel) sorted as function of TSG-GOSUD-Research-vessel SSS values a), TSG-GOSUD-Research-vessel SST b), ASCAT Wind speed c), CMORPH rain rate d) and distance to coast (e). In all plots the mean and STD of ΔSSS for each bin is indicated by the red curves and black vertical thick bars (±1 STD)

In Figures 12 and 13, we focus on sub-datasets of the match-up differences ΔSSS (Satellite - in situ) between SMAP-L3-JPL-V4-8DAY-RUNNING-60KM and TSG-GOSUD-Research-vessel for the following specific geophysical conditions:

- **C1**:if the local value at in situ location of estimated rain rate is high (ie. $>$ 10 mm/h) and mean daily wind is low (ie. $<$ 5 m/s).
- **C2**:if the prior 10-days history of the rain and wind at in situ location show high (ie.$>$ 5

mm/h) and low (ie.< 5 m/s) median values, respectively.

- **C3**:if both C1 and C2 are met.
- **C6**:if the in situ data is located where the climatological sss standard deviation is high (ie. above > 0.2).

For each of these conditions, the temporal mean (gridded over spatial boxes of size 1°x1°) and the histogram of the difference ΔSSS (Satellite - in situ) are presented.

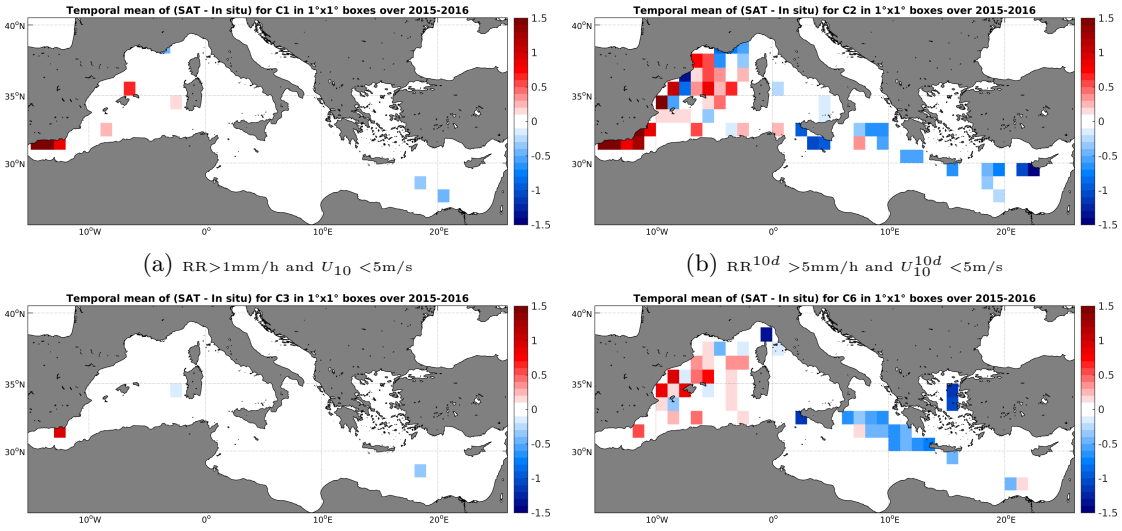

(a) RR>1mm/h and U_{10} <5m/s

(b) RR^{10d} >5mm/h and U_{10}^{10d} <5m/s

(c) C1 U C2

(d) Locations where WOA2013 SSS STD>0.2

Figure 12: Temporal mean gridded over spatial boxes of size 1°x1° of ΔSSS (SMAP-L3-JPL-V4-8DAY-RUNNING-60KM - TSG-GOSUD-Research-vessel) for 4 different subdatasets corresponding to:RR>1mm/h and U_{10} <5m/s (a), RR^{10d} >5mm/h and U_{10}^{10d} <5m/s (b), C1 U C2 (c),Locations where WOA2013 SSS STD>0.2 (d).

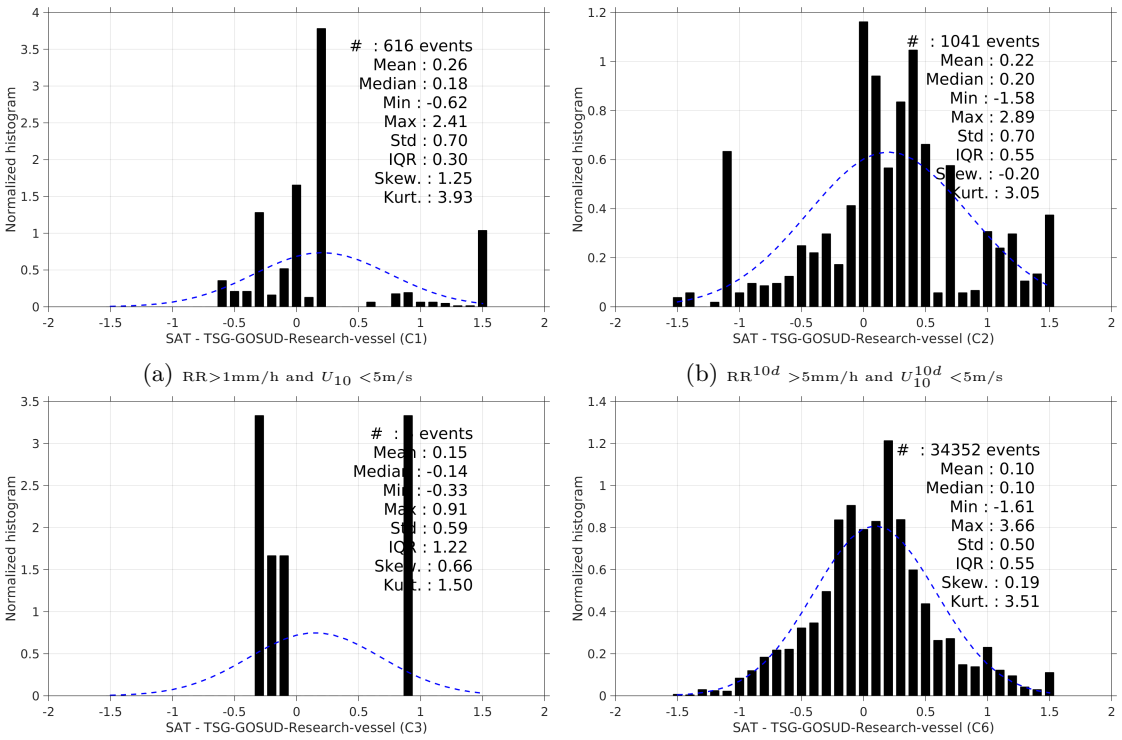

(a) RR>1mm/h and U_{10} <5m/s

(b) RR^{10d} >5mm/h and U_{10}^{10d} <5m/s

(c) C1 U C2

(d) Locations where WOA2013 SSS STD>0.2

Figure 13: Normalized histogram of ΔSSS (SMAP-L3-JPL-V4-8DAY-RUNNING-60KM - TSG-GOSUD-Research-vessel) for 6 different subdatasets corresponding to: RR>1mm/h and U_{10} <5m/s (a), RR^{10d} >5mm/h and U_{10}^{10d} <5m/s (b), C1 U C2 (c), Locations where WOA2013 SSS STD>0.2 (d).

4 Summary

Table 1 presents statistics (mean, median, standard deviation, root mean square and inter-quantile range) of the match-up differences ΔSSS (Satellite - in situ) between SMAP-L3-JPL-V4-8DAY-RUNNING-60KM and TSG-GOSUD-Research-vessel derived over the Mediterranean Sea Pi-MEP region and for the full satellite product period and for the following conditions:

- all: All the match-up pairs satellite/in situ SSS values are used to derive the statistics
- C1: only pairs where RR>1mm/h and U_{10} <5m/s
- C2: only pairs where RR^{10d} >5mm/h and U_{10}^{10d} <5m/s
- C3: only pairs where C1 U C2
- C6: only pairs at Locations where WOA2013 SSS STD>0.2
- C7a: only pairs with a distance to coast < 150 km.
- C7b: only pairs with a distance to coast in the range [150, 800] km.
- C7c: only pairs with a distance to coast > 800 km.

- C8a: only pairs where SST is $< 5°C$.
- C8b: only pairs where SST is in the range [5, 28]°C.
- C8c: only pairs where SST is $> 28°C$.
- C9a: only pairs where SSS is < 33.
- C9b: only pairs where SSS is in the range [33, 37].
- C9c: only pairs where SSS is > 37.

Table 1: Statistics of ΔSSS (Satellite - TSG-GOSUD-Research-vessel)

Condition	#	Median	Mean	Std	RMS	IQR
all	91268	0.02	0.04	0.61	0.61	0.49
C1	616	0.18	0.26	0.70	0.74	0.30
C2	1041	0.20	0.22	0.70	0.73	0.55
C3	6	-0.14	0.15	0.59	0.56	1.22
C6	34352	0.10	0.10	0.50	0.51	0.55
C7a	84034	0.01	0.03	0.62	0.62	0.47
C7b	7234	0.18	0.11	0.37	0.39	0.51
C7c	0		NaN	NaN	NaN	NaN
C8a	0		NaN	NaN	NaN	NaN
C8b	0		NaN	NaN	NaN	NaN
C8c	0		NaN	NaN	NaN	NaN
C9a	119	5.55	6.24	1.96	6.53	2.46
C9b	3541	0.72	0.94	0.88	1.29	0.96
C9c	87608	0.00	-0.01	0.51	0.51	0.46

For the same conditions, Table 2 presents statistics of ΔSSS (Satellite - ISAS). Only ISAS SSS values with PCTVAR<80% are used to derive the statistics.

Table 2: Statistics of ΔSSS (Satellite - ISAS)

Condition	#	Median	Mean	Std	RMS	IQR
all	91268	0.03	0.03	0.61	0.51	0.51
C1	616	-0.24	0.05	0.77	0.77	0.11
C2	1041	0.15	0.14	0.62	0.64	0.64
C3	6	-0.33	0.04	0.79	0.72	1.64
C6	34352	0.03	0.06	0.47	0.47	0.51
C7a	82690	0.02	0.02	0.52	0.52	0.49
C7b	7234	0.18	0.15	0.37	0.40	0.47
C7c	0		NaN	NaN	NaN	NaN
C8a	0		NaN	NaN	NaN	NaN
C8b	0		NaN	NaN	NaN	NaN
C8c	0		NaN	NaN	NaN	NaN
C9a	119	-1.17	-1.09	0.23	1.11	0.35
C9b	3506	0.03	0.12	1.09	1.10	1.68
C9c	86299	0.03	0.03	0.47	0.47	0.49

References

Abderrahim Bentamy and Denis Croize Fillon. Gridded surface wind fields from Metop/ASCAT measurements. *Int. J. Remote Sens.*, 33(6):1729–1754, March 2012. ISSN 1366-5901. doi: 10.1080/01431161.2011.600348.

Abderrahim Bentamy, Semyon A. Grodsky, James A. Carton, Denis Croizé-Fillon, and Bertrand Chapron. Matching ASCAT and QuikSCAT winds. *J. Geophys. Res.*, 117(C2), February 2012. ISSN 0148-0227. doi: 10.1029/2011JC007479. C02011.

Jaqueline Boutin, Y. Chao, W. E. Asher, T. Delcroix, R. Drucker, K. Drushka, N. Kolodziejczyk, T. Lee, N. Reul, G. Reverdin, J. Schanze, A. Soloviev, L. Yu, J. Anderson, L. Brucker, E. Dinnat, A. S. Garcia, W. L. Jones, C. Maes, T. Meissner, W. Tang, N. Vinogradova, and B. Ward. Satellite and In Situ Salinity: Understanding Near-Surface Stratification and Sub-footprint Variability. *Bull. Am. Meterol. Soc.*, 97(8):1391–1407, 2016. ISSN 1520-0477. doi: 10.1175/bams-d-15-00032.1.

Clément de Boyer Montégut, Gurvan Madec, A. S. Fischer, A. Lazar, and D. Ludicone. Mixed layer depth over the global ocean: An examination of profile data and a profile-based climatology. *J. Geophys. Res.*, 109(C12):C12003, December 2004. ISSN 0148-0227. doi: 10.1029/2004jc002378.

Clément de Boyer Montégut, Juliette Mignot, Alban Lazar, and Sophie Cravatte. Control of salinity on the mixed layer depth in the world ocean: 1. General description. *J. Geophys. Res.*, 112(C6):C06011, June 2007. ISSN 0148-0227. doi: 10.1029/2006jc003953.

Ralph R. Ferraro. Ssm/i derived global rainfall estimates for climatological applications. *J. Geophys. Res.*, 1021:16715–16736, 07 1997. doi: 10.1029/97JD01210.

Ralph R. Ferraro, Fuzhong Weng, Norman C. Grody, and Limin Zhao. Precipitation characteristics over land from the NOAA-15 AMSU sensor. *Geophys. Res. Lett.*, 27(17):2669–2672, 2000. doi: 10.1029/2000GL011665.

Fabienne Gaillard, E. Autret, V. Thierry, P. Galaup, C. Coatanoan, and T. Loubrieu. Quality Control of Large Argo Datasets. *J. Atmos. Oceanic Technol.*, 26(2):337–351, 2012/10/10 2009. doi: 10.1175/2008JTECHO552.1.

Fabienne Gaillard, Denis Diverres, Stéphane Jacquin, Yves Gouriou, Jacques Grelet, Marc Le Menn, Joelle Tassel, and Gilles Reverdin. Sea surface temperature and salinity from French research vessels, 2001-2013. *Sci. Data*, 2(150054), October 2015. ISSN 2052-4463. doi: 10.1038/sdata.2015.54.

Fabienne Gaillard, Thierry Reynaud, Virginie Thierry, Nicolas Kolodziejczyk, and Karina von Schuckmann. In Situ-Based Reanalysis of the Global Ocean Temperature and Salinity with ISAS: Variability of the Heat Content and Steric Height. *J. Clim.*, 29(4):1305–1323, February 2016. ISSN 1520-0442. doi: 10.1175/jcli-d-15-0028.1.

Robert J. Joyce, John E. Janowiak, Phillip A. Arkin, and Pingping Xie. CMORPH: A Method that Produces Global Precipitation Estimates from Passive Microwave and Infrared Data at High Spatial and Temporal Resolution. *J. Hydrometeorol.*, 5(3):487–503, June 2004. ISSN 1525-7541. doi: 10.1175/1525-7541(2004)005⟨0487:camtpg⟩2.0.co;2.

Nicolas Kolodziejczyk, Gilles Reverdin, and Alban Lazar. Interannual Variability of the Mixed Layer Winter Convection and Spice Injection in the Eastern Subtropical North Atlantic. *J. Phys. Oceanogr.*, 45(2):504–525, Feb 2015. ISSN 1520-0485. doi: 10.1175/jpo-d-14-0042.1.

Christian Kummerow, Y. Hong, W. S. Olson, S. Yang, R. F. Adler, J. McCollum, R. Ferraro, G. Petty, D-B. Shin, and T. T. Wilheit. The Evolution of the Goddard Profiling Algorithm (GPROF) for Rainfall Estimation from Passive Microwave Sensors. *J. Appl. Meteorol.*, 40(11): 1801–1820, 2001. doi: 10.1175/1520-0450(2001)040⟨1801:TEOTGP⟩2.0.CO;2.